buildings

MDPI

Article

Feasibility of Multi-Zone Simulation for Estimating Contributions of Outdoor Particulate Pollution to Indoor Particulate Matter Concentration

Byung-Hee Lee [1] and Seung-Hyo Baek [2,*]

[1] Land & Housing Institute, Daejeon 34047, Republic of Korea
[2] Division of Architecture, Mokwon University, Daejeon 35349, Republic of Korea
* Correspondence: shbaek@mokwon.ac.kr

Abstract: As concerns about the health effects of particulate matter (PM) are growing, controlling indoor PM has become vital for ensuring occupants' health. Active strategies, such as air purification and high-performance filtering, are widely implemented to control indoor PM. However, passive strategies, including air-tightness and compartmentalization, are promising alternatives, as demonstrated by recent studies. To enhance the implementation of passive strategies, an appropriate evaluation method for passive designs must be established. The objective of this study was to investigate whether a multi-zone-based method is suitable for the evaluation of passive strategies. Multi-zone simulations were performed for four seasons, and indoor/outdoor concentration (I/O) ratios were obtained for the exterior, interior, and corridor on every floor of the reference building. The I/O ratios at different locations indicated that the outdoor particle transport in the building was accurately estimated according to the airflow rate and path. Moreover, in addition to the effects of changes in the outdoor temperature on PM transport through the building envelope, the particle size is a significant factor affecting indoor PM concentrations. The results of this study indicated that the multi-zone method can effectively estimate the number of outdoor particles that penetrate the building envelope in different seasons and the indoor particle concentration at different indoor locations.

Keywords: particulate matter; airflow; multi-zone simulation; indoor/outdoor concentration (I/O) ratio

check for updates

Citation: Lee, B.-H.; Baek, S.-H. Feasibility of Multi-Zone Simulation for Estimating Contributions of Outdoor Particulate Pollution to Indoor Particulate Matter Concentration. *Buildings* **2023**, *13*, 673. https://doi.org/10.3390/buildings13030673

Academic Editor: Christopher Yu-Hang Chao

Received: 28 December 2022
Revised: 20 January 2023
Accepted: 28 February 2023
Published: 3 March 2023

Copyright: © 2023 by the authors. Licensee MDPI, Basel, Switzerland. This article is an open access article distributed under the terms and conditions of the Creative Commons Attribution (CC BY) license (https://creativecommons.org/licenses/by/4.0/).

1. Introduction

As the health effects of particulate matter (PM), including respiratory disease, heart attacks, and premature death have been proven, interest in controlling PM has significantly increased over the past decades [1–7]. Moreover, as people spend more than 80% of their time indoors, indoor air pollution control is as important as outdoor control [8–11]. The indoor PM concentration can be increased by various factors, among which, the penetration of outdoor PM due to infiltration and mechanical ventilation is a major factor. Other sources of indoor PM include cooking and combustion activities [12–14]. Recent studies proved that the inflow of PM from adjacent rooms can significantly increase the indoor PM concentration [13,15–17]. Methods for reducing the indoor PM concentration include minimizing the penetration of outdoor PM and controlling indoor PM generation.

To reduce the indoor PM concentration, active strategies based on mechanical equipment are commonly applied to buildings, one of which involves the installation of air purifiers in rooms. In buildings with air-handling units or mechanical ventilation systems, installing additional high-efficiency particulate air filters in the systems can eliminate a large amount of PM in the inflow air. Although active strategies can reduce indoor PM, they are expensive. Moreover, the operation of active systems consumes more energy; consequently, more PM is emitted into the atmosphere.

Recent studies indicated that passive strategies are effective for controlling indoor PM [18–21]. In these studies, authors examined whether the air-tightness of building envelopes can reduce the indoor PM concentration. Studies suggested that strong envelope air-tightness can reduce the indoor PM concentration [18,21]. Others suggested that compartmentalization can mitigate the movement of $PM_{2.5}$ in buildings. In most studies, compartmentalization was applied only for $PM_{2.5}$ generated by smoking activities; however, compartmentalization can also be applied to reduce the amount of PM generated by outdoor smoking [16,22,23]. Appropriate passive strategies, such as envelope air-tightness and compartmentalization, can reduce the indoor PM concentration, leading to energy-efficient indoor PM control.

Although several studies demonstrated the effectiveness of passive strategies for reducing indoor PM concentrations, these strategies may not be effective for all buildings. Therefore, further evaluation is necessary to determine the most suitable passive strategy for a building. Unfortunately, the complex mechanism of PM transfer in buildings renders this process challenging. Thus, an appropriate method for evaluating the effects of passive strategies on indoor PM concentrations before their implementation is crucial.

In this regard, indoor PM evaluation methods were proposed [6], most of which were measurement-based approaches. Outdoor and indoor PM concentrations were measured, and indoor/outdoor concentration (I/O) ratios were calculated [24–27]. The I/O ratio, which is a simple index, is widely used to evaluate indoor PM concentrations. However, in studies using I/O ratios, it is typically assumed that a certain indoor concentration level represents all indoor locations. This assumption is valid for small buildings, but not for medium-sized or large buildings. Furthermore, it is unsuitable for examining the effects of compartmentalization on the PM concentration in each zone of the building.

In addition to its simple assumption from a spatial perspective, some studies assumed that a temporal state is simplified to a steady state. This assumption also entails certain constraints in evaluating the impact of passive strategies on decreasing the indoor PM concentration. Most importantly, the transient effects of weather and the outdoor PM concentration cannot be reflected. The wind speed and outdoor temperature significantly affect the infiltration rate, influencing the number of penetrating outdoor particles [28]. If dynamic conditions such as changes in wind speed and outdoor temperature are not considered in the evaluation, the penetration of outdoor particles cannot be accurately estimated. Consequently, the amount of indoor particulate reduction that can be achieved using passive strategies, such as air-tightness, cannot be accurately evaluated. In addition to weather effects, a change in outdoor particulate pollution is considered in the temporal state. The generation of outdoor particles tends to increase in winter, owing to the increased demand for domestic heating. Therefore, the steady-state assumption is unsuitable for modeling seasonal changes in outdoor PM pollution.

To overcome the limitations of the aforementioned simplified evaluation method for indoor particle concentrations, several studies employed computational fluid dynamics (CFD) [29–33]. The entire indoor space is fully discretized, allowing the estimation of the particle concentration at any location. CFD models provide the detailed spatial distribution and temporal evolution of the indoor particle concentration by simultaneously solving corresponding conservation equations [29]. Despite its capability, the use of CFD in the design stage is impractical. Meshing and calculation in CFD are time-consuming, even when advanced computing resources are available. For iteratively evaluating different passive strategies, a simpler method should be developed.

Recent studies proposed an airflow-network-based indoor PM evaluation method [34–37]. This method evaluated the effects of individual sources on the indoor PM concentration by dividing a large space into small compartments and calculating the airflow rates through network airflow paths as well as the mean particle concentration in individual zones [29]. According to the findings of these studies, this method is suitable for estimating indoor PM concentrations. Therefore, in the present study, we investigated the effectiveness of the method for evaluating passive strategies during the design stage. The investigation aimed

to determine whether this method can estimate indoor PM concentrations at different indoor locations from a spatial perspective and consider seasonal changes in outdoor weather and PM concentrations from a temporal perspective.

2. Factors Related to Particle Transport from Outdoors to Indoors

2.1. Mechanism of Indoor Particle Transport

PM suspended in indoor air comprises particles from both outdoor and indoor sources. The indoor PM concentration is determined by a series of processes, such as air exchange between indoor and outdoor environments, deposition, resuspension, and generation, as shown in Figure 1. These processes can be expressed using a mass-balance equation based on material conservation:

$$\frac{d}{dt}N_{k,i} = \frac{1}{V_k}\sum_m Q_{mk}P_{m.i}N_{out,i} - \frac{1}{V_k}Q_{k,removed}N_{k,i} + \frac{1}{V_k}\sum_i\left(Q_{jk}N_{j,i} - Q_{kj}N_{k,i}\right) - \frac{1}{V_k}\sum_j A_{kj}\nu_{kj,d,i}N_{k,i} + \frac{1}{V_k}\sum_j f_{k,j,i}A_{k,j}\lambda_{kj,re,i}B_{kj,i} + G^E_{k,i} \quad (1)$$

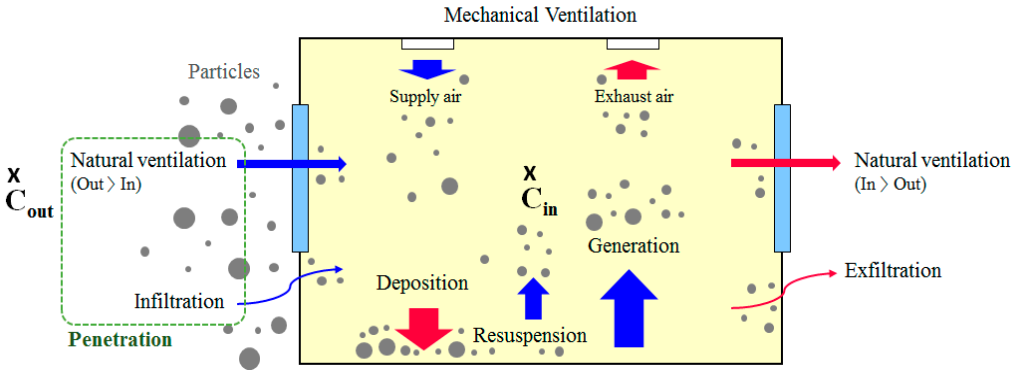


Figure 1. Mechanism of particle penetration and transport.

The equation for the indoor PM concentration consists of six terms: (1) $\frac{1}{V_k}\sum_m Q_{mk}P_{m.i}N_{out,i}$ represents the penetration, filtration, and infiltration during indoor-outdoor air exchange; (2) $\frac{1}{V_k}Q_{k,removed}N_{k,i}$ represents the exfiltration from the indoor space k; (3) $\frac{1}{V_k}\sum_i\left(Q_{jk}N_{j,i} - Q_{kj}N_{k,i}\right)$ represents the internal air exchange between indoor spaces; (4) $\frac{1}{V_k}\sum_j A_{kj}\nu_{kj,d,i}N_{k,i}$ represents the deposition of suspended particles on indoor surfaces; (5) $\frac{1}{V_k}\sum_j f_{k,j,i}A_{k,j}\lambda_{kj,re,i}B_{kj,i}$ represents the resuspension of deposited particles; and (6) $G^E_{k,i}$ represents the new particle emission and generation.

As shown in Figure 2, assuming no resuspension of particles and no indoor sources, three factors affect particle movement indoors: the penetration coefficient and deposition rate, indoor–outdoor air exchange rate, and outdoor particle concentration.

2.2. Penetration Coefficient and Deposition Rate

The particle penetration coefficient and deposition rate provide a direct relationship between air cleanliness and contamination risk [5,6,24,36,38]. Outdoor air enters a building through cracks in the building envelope generated by multiple driving forces [39,40]. Some airborne particles may accumulate on crack surfaces without passing through the inlet path [6]. The penetration coefficient refers to the partial penetration of particles from outdoors to indoors due to the infiltrating airflow [16,40].

Particle deposition refers to the spontaneous attachment of suspended particles to these surfaces [16,41]. Particle deposition on indoor surfaces involves several processes, which are dependent on particle size [16,36]. Brownian diffusion is an important type of motion observed in ultrafine particles. Gravitational precipitation, which can be increased

by inertial collisions, is a key mechanism for coarse particles [42]. Particles are deposited on surfaces as they penetrate or are filtered from outdoors to indoors [5].

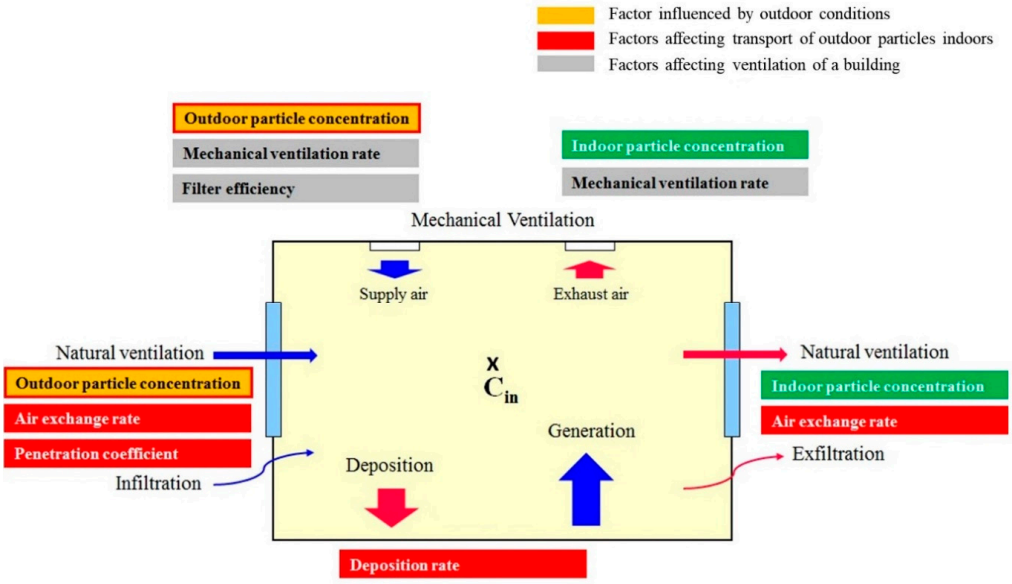


Figure 2. Factors related to particle transport from outdoors to indoors.

2.3. Outdoor Air Exchange Rate

The air exchange rate refers to the amount of airflow per hour. It is the measure of the air volume added to or removed from a room per hour divided by the volume of the space. The driving forces of airflow in a building are the buoyancy induced by wind pressure, indoor–outdoor temperature difference, and indoor–outdoor pressure difference caused by the mechanical ventilation system. At least one of these factors is needed to generate airflow.

Airflow from outdoors to indoors is the primary driving force for particle transport [43]. In winter, outdoor air flows indoors through the lower levels of a building and generates an upward airflow to the upper levels owing to the indoor–outdoor pressure difference. This implies that when the outdoor particulate pollution level is high during the cold season, outdoor particles can flow into a building through airflow. These particles spread to the upper levels of the building through the stack effect, i.e., the updraft caused by the temperature difference between outdoors and indoors. Thus, the indoor PM concentration may be affected by the air pollution level.

2.4. Outdoor Particulate Pollution

Air pollution is an important social issue in Korea. The average outdoor PM_{10} and $PM_{2.5}$ concentrations were 40 and 23 μg m^{-3}, respectively, in Seoul in 2018 [44]. Considering that the average annual outdoor PM_{10} concentration in major developed cities, such as Tokyo and New York, is smaller than 30 μg m^{-3} [45], the domestic outdoor PM_{10} concentration in Seoul is extremely high. In 2016, there was a $PM_{2.5}$ warning for 13 d, and the average daily outdoor $PM_{2.5}$ concentration in Seoul was 57.1 μg m^{-3}. In 2018, there was a $PM_{2.5}$ warning for 20 d, and the average daily outdoor $PM_{2.5}$ concentration in Seoul was 65.6 μg m^{-3}.

According to Equation (1), the outdoor PM concentration is the primary factor that determines the indoor PM concentration. One of the main methods implemented for indoor air quality (IAQ) management in Korea is natural ventilation, because the outdoor particulate pollution level in Korea was low in the past. However, currently, ventilation using outdoor air cannot ensure satisfactory IAQ. In particular, when the outdoor PM concentration is high, such as during winter, outdoor particles are transported indoors through ventilation, increasing the indoor PM concentration. Because the outdoor PM

concentrations affects the indoor PM concentrations, conventional IAQ management techniques such as natural ventilation are no longer viable options given the elevated outdoor PM levels.

3. Methods

3.1. Simulation Modeling

Factors affecting indoor PM concentrations include the penetration coefficient, deposition coefficient, and air exchange rate, assuming that the particles are resuspended and no indoor sources are present. Simulation modeling that reflects changes in major influencing factors can accurately predict the number and path of particles penetrating from the outdoors.

As shown in Figure 3, a multi-zone simulation model was used to evaluate the airflow and transport of particles from outdoors to indoors. The CONTAMW simulation program was used to analyze the airflow network model and pollutant transport [46]. This program was widely used in IAQ research focusing on various pollutant transport problems. Recently, researchers used CONTAMW to evaluate particle transport issues, including not only airborne contaminants but also infectious viruses [46–50]. Detailed governing equations for CONTAMW can be found in Equation (1) [51].

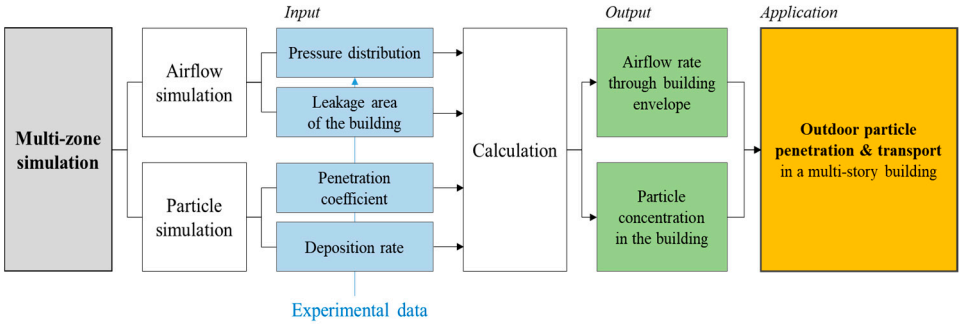


Figure 3. Conceptual diagram of multi-zone simulation modeling.

For studies using simulation models, the number of particles moving from outdoors to indoors can be quantified regardless of the outdoor conditions, and factors such as the air exchange rate and particle diameter can be evaluated. However, because the data related to the input values of the simulation models were insufficient in this study, an additional process was necessary to ensure the reliability of the input values.

For the particle transport simulation, the two main parameters—the penetration coefficients and deposition rates—were determined via field tests. CONTAMW does not provide a model for particle penetration, although built-in models can account for particle deposition loss. The input value was modified in CONTAMW to evaluate the particle penetration as a function of the airflow rate and particle penetration coefficient. A conceptual diagram of the simulation approach is presented in Figure 3.

To calculate the amount of airflow in each room in the airflow network model, the leakage-area data of the reference building component are required. In this study, the pressurization/depressurization method using a blower door based on the International Organization for Standardization (ISO) 9972 was used to obtain these data. To verify the airflow model implemented in the CONTAMW program, the indoor and outdoor pressure distributions of the reference building were measured and compared with the simulation results.

The reference building components included entrance doors, interior doors, stairwell and elevator doors, exterior and interior walls, and windows. The blower door device used in the field measurements was a Retrotec 3101 blower door measuring system (Retrotec, USA) with a fan. The maximum airflow rate was 14,100 m^3 h^{-1} at 50 Pa, and the flow accuracy was ±5%.

In this study, the CONTAMW model was used to estimate the airflow according to the air leakage data for each zone in the reference building. Additionally, it was used to calculate the amount of indoor PM transport in the interzonal airflow. However, the particle deposition on indoor surfaces and penetration through the exterior and interior walls of the reference building could not be directly implemented using this model. Thus, several input values in the CONTAMW model were modified to incorporate these two key parameters when estimating indoor PM concentrations [52].

The penetration coefficient and deposition rate were the primary particle simulation input data. The penetration coefficient represents the fraction of particles that can infiltrate indoor spaces [53]. The deposition rate is the rate of particle loss, which occurs throughout the particle transport to surfaces, due to sinking [54]. As shown in Figure 4, the deposition rate and penetration coefficient were measured using a natural decay test in the reference building [53]. The experimental values were used as essential parameters in the simulation.

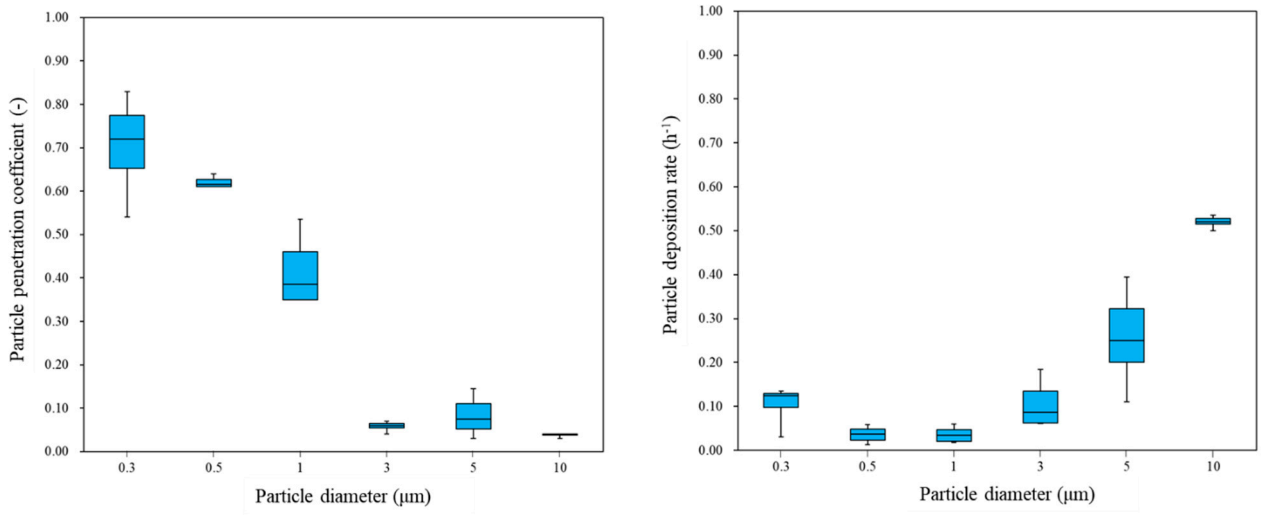


Figure 4. (**a**) Penetration coefficients and (**b**) deposition rates of size-resolved particles.

Before the test, the reference room was cleaned, and the windows were opened to allow outdoor PM to flow indoors, increasing the indoor PM. Mixing fans were operated for 1 h to achieve good mixing conditions in the test space. After turning off the fans and closing all the doors and windows, the indoor and outdoor PM number concentrations were measured using two identical optical particle counters (OPCs, TSI 9306-v2, TSI, USA) for a natural decay test.

Particle movements such as penetration, diffusion, and transport are affected by the particle size. In this study, particles, which were defined as having a diameter of smaller than 10 μm, were classified into six groups (0.3, 0.5, 1, 3, 5, and 10 μm) according to their diameter, in accordance with ISO 14644-1 (ISO 2015b). The OPC continuously counted the particles in these groups at a flow rate of 0.17 m^3 h^{-1} with an accuracy of ±5%. The outdoor PM number concentration was measured from the center of the roof, and the indoor PM number concentration was measured 1 m from the exterior window and 1.2 m from the floor. The indoor and outdoor PM counts were recorded every 10 min during the test period.

3.2. Description of Reference Building and Simulation Conditions

As shown in Figure 5, a multi-story, multi-zone building was selected as the reference building, considering the common office building types in Korea. Particles transported from outdoors to indoors could spread throughout the building via vertical paths, such as elevators and staircases. The reference building was a medium-sized office building located in Seoul, Korea. It had five stories above ground and two stories below ground, and

its height was approximately 23 m. The first and second basement levels of the building were parking lots, and the second to fifth floors above the ground were offices.

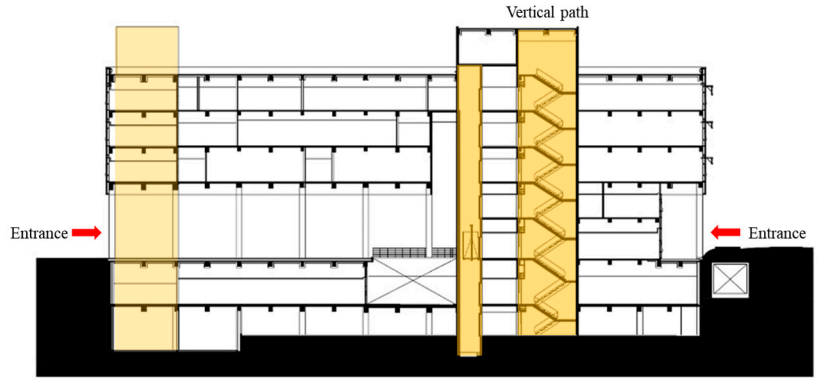
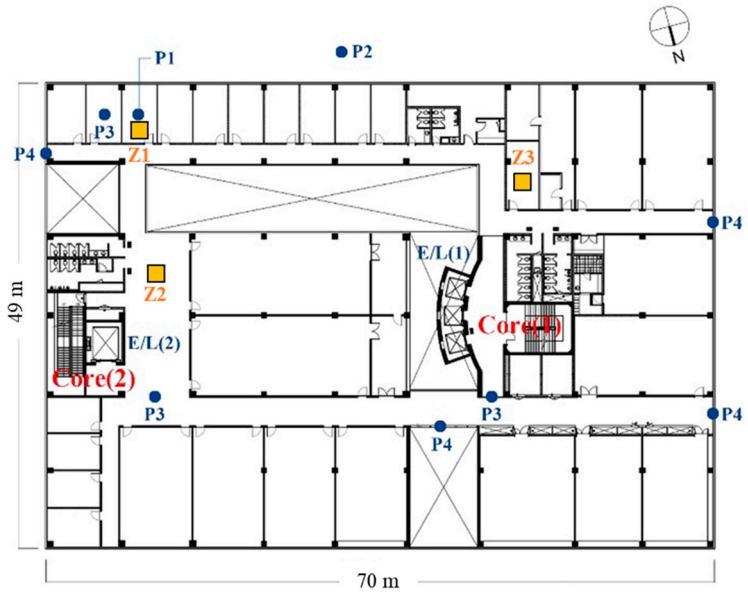


Figure 5. Cross-section of the reference building.

The typical floor plan and measurement points of the reference building are shown in Figure 6. In the reference building, the rooms, such as an office or a meeting rooms, consisted of similar sets of building envelope systems, interior finishes, and furniture. The exterior of this building was designed and installed as a curtain wall system. Because the test building was constructed in 2013, the leakage areas for the exterior and interior walls were expected to be uniform. The test building was a small-to-medium-sized office building with natural ventilation throughout the indoor spaces. The mechanical ventilation systems were installed only in the basement of the building.



P1: Measurement point for particle concentration
P2: Measurement point for outdoor conditions
P3: Measurement point for indoor temperature and absolute pressure
P4: Measurement point for pressure difference at exterior
Z1: Exterior zone
Z2: Corridor
Z3: Interior zone

Figure 6. Floor plan of the reference building.

The simulation was conducted for days in different seasons between January and December when the outdoor PM concentrations were high. As shown in Table 1, the four seasons were representative of spring, summer, autumn, and winter in Korea. Input

variables such as the ambient temperature, relative humidity, wind velocity, and wind direction in the different seasons were measured for the reference building. It was assumed that all openings, including doors and windows, were closed as usual.

Table 1. Simulation input data for the outdoor and indoor environmental conditions.

	Case 1	**Case 2**	**Case 3**	**Case 4**
Season	Spring	Summer	Autumn	Winter
Outdoor temperature (°C)	12.0	24.3	14.4	–0.5
Relative humidity (%)	59	74	65	59
Wind velocity (m s^{-1})	2.7	2.2	2.0	2.4
Wind direction (°)	270	68	45	293
Indoor temperature (°C)	23.0	25.0	23.0	22.0

We hypothesized that outdoor air and PM can enter in parts of the test building. These particles can be transported through vertical and horizontal spaces, particularly when the outdoor PM concentration is high. The outdoor size-resolved PM concentration was used as the measured value during periods of high air pollution in South Korea. As shown in Table 2, the total outdoor PM mass concentration was set within the range of 21–125 μg m^{-3} per day. To estimate solely the effect of outdoor particles on the indoor environment, particle sources such as office equipment and occupant activities were ignored in the indoor spaces.

Table 2. Size-resolved outdoor PM mass concentrations.

PM Diameter (μm)	**Mass Concentration (μg m^{-3})**			
	Case 1	**Case 2**	**Case 3**	**Case 4**
0.3	14.4	5.0	9.0	19.6
0.5	9.6	3.3	6.0	13.1
1.0	14.4	5.0	9.0	19.6
3.0	4.7	1.5	3.0	13.8
5.0	14.1	4.6	8.9	41.3
10.0	6.3	2.1	4.0	18.4
Total	63.5	21.5	39.8	125.6

4. Simulation Results

4.1. Airflow Results

The pressure distributions and air exchange rates for different seasons were estimated using a multi-zone simulation model. Herein, the air exchange rate refers to the infiltration rate. The simulation was conducted with doors and windows closed. The seasonal pressure distributions and infiltration rates were compared to evaluate the effects of external environmental conditions on the airflow and transport of outdoor particles.

Figure 7a–d shows the vertical pressure distribution of the test building. A difference between the indoor and outdoor pressures was observed in spring, autumn, winter, and summer, and the airflow was affected by the pressure difference. Thus, in spring, autumn, and winter, particles were transported by airflow from the lower floors, traveled through the vertical paths, and flowed to the upper floors owing to the stack effect. In contrast, in summer, outdoor particles in the indoor air flowed from the upper part, descended through the vertical paths, and flowed out to the lower part.

Among the external environmental factors that affected the infiltration rate, the wind direction and wind speed did not significantly affect the infiltration rate, because the seasonal values did not differ. Thus, the pressure difference due to the temperature difference between the indoor and outdoor environments was the driving force for air movement in the reference building. In winter, the infiltration rate was the highest because the temperature difference between indoors and outdoors was larger than those in the other seasons.

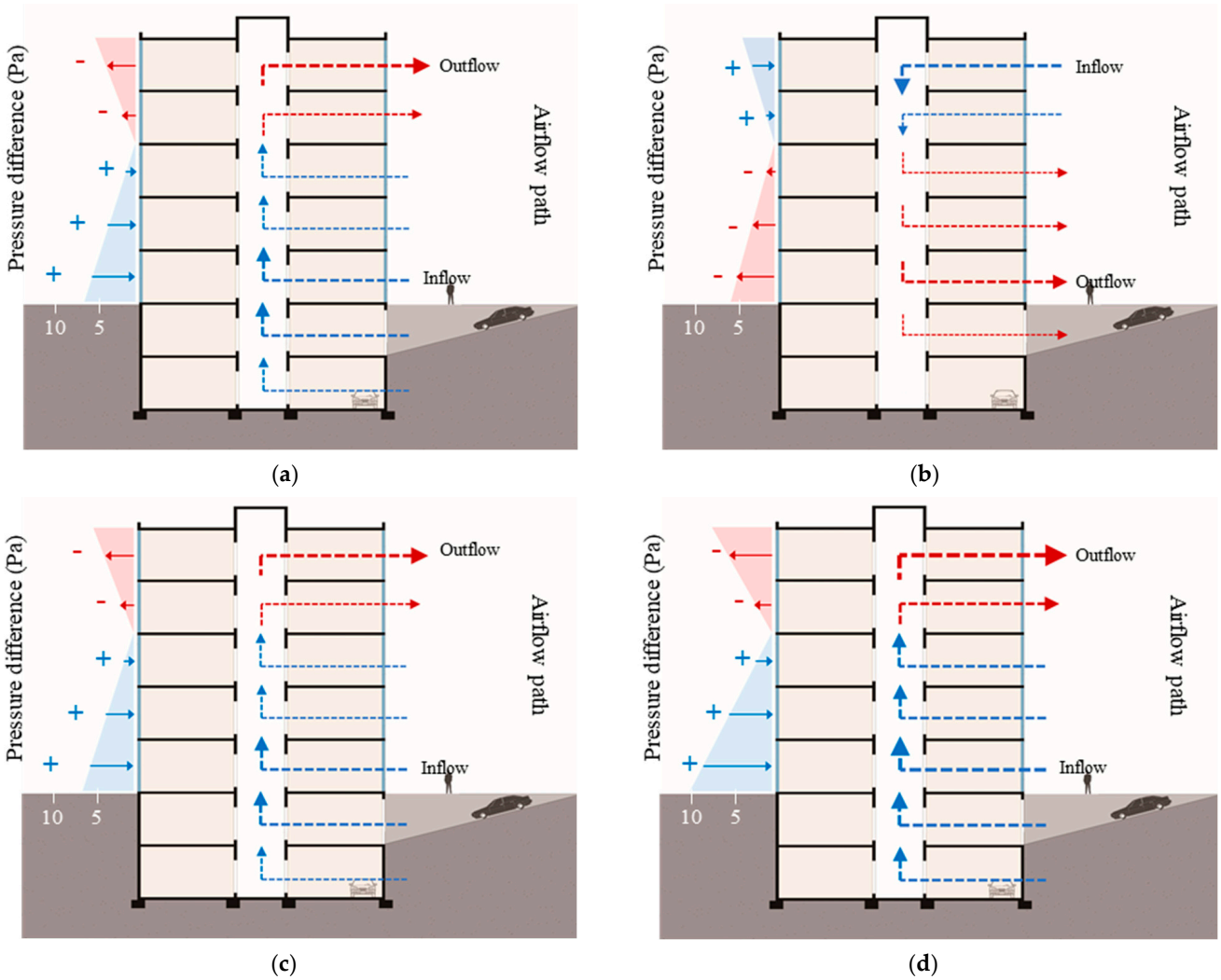


Figure 7. Pressure distribution and airflow path in the reference building: (**a**) case 1, spring; (**b**) case 2, summer; (**c**) case 3, autumn; (**d**) case 4, winter.

The differences between the indoor and outdoor pressures generated on the first and highest floors in winter were approximately 10 and −5 Pa, respectively. In general, the pressure difference between the indoor and outdoor environments was within the range of 0–5 Pa for a single-story building. The maximum pressure difference of 10 Pa indicated that the building allowed airflow to transport particles from outdoors to indoors.

As shown in Figure 8, the airflow rate in spring ranged from 1.89 to 1.92 air changes per hour (ACH) on the lower floors and from −0.30 to −0.38 ACH on the upper floors. These values were similar to those for autumn. In winter, the airflow rate ranged from 1.97 to 3.10 ACH on the lower floors and from −0.46 to −0.62 ACH on the upper floors, and the airflow direction was similar to those in spring and autumn. In summer, the airflow rate on the lower floors ranged from −0.53 to −1.63 ACH, whereas that on the upper floor ranged from 0.06 to 0.21 ACH, and the airflow path differed from those in the other seasons. These results indicated that the airflow direction and airflow rate of each floor varied with respect to the season.

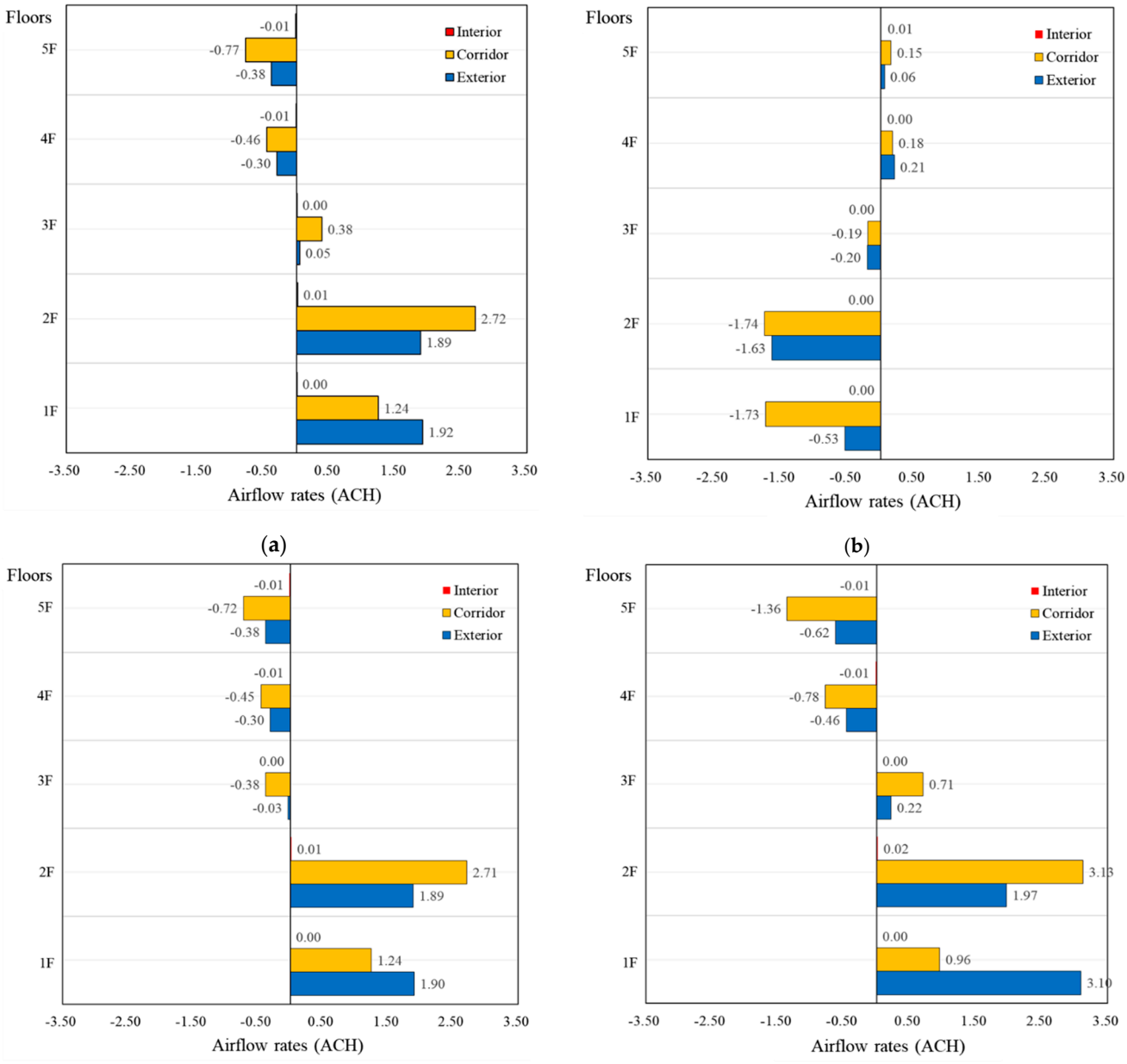


Figure 8. Airflow rates in the reference building: (**a**) case 1, spring; (**b**) case 2, summer; (**c**) case 3, autumn; (**d**) case 4, winter.

4.2. Particle Results (I): Amount of Outdoor Particle Penetration

To analyze the penetration of outdoor particles, the number of outdoor particles that infiltrated the exterior of the building was estimated. The results are shown in Figure 9a–d. The number of outdoor particles that penetrated the reference-building envelope was defined as the product of the penetration coefficient and the air exchange rate, as follows:

$$A_i = P_i \times a \tag{2}$$

In the analysis of the inflow and outflow of particles from the outdoors, (+) and (−) were used to express the directions of inflow and outflow. For each season, the inflow and outflow of outdoor particles were similar to the airflow pattern. In spring, autumn, and winter, outdoor particles flowed through the lower floor and out through the upper floor, whereas in summer, particles in the air that reached through the upper floor flowed out

through the lower floor. Additionally, particles entering the building move to other spaces of the building, and some particles were lost because of penetration and deposition. The amount of particle loss depended on the particle size.

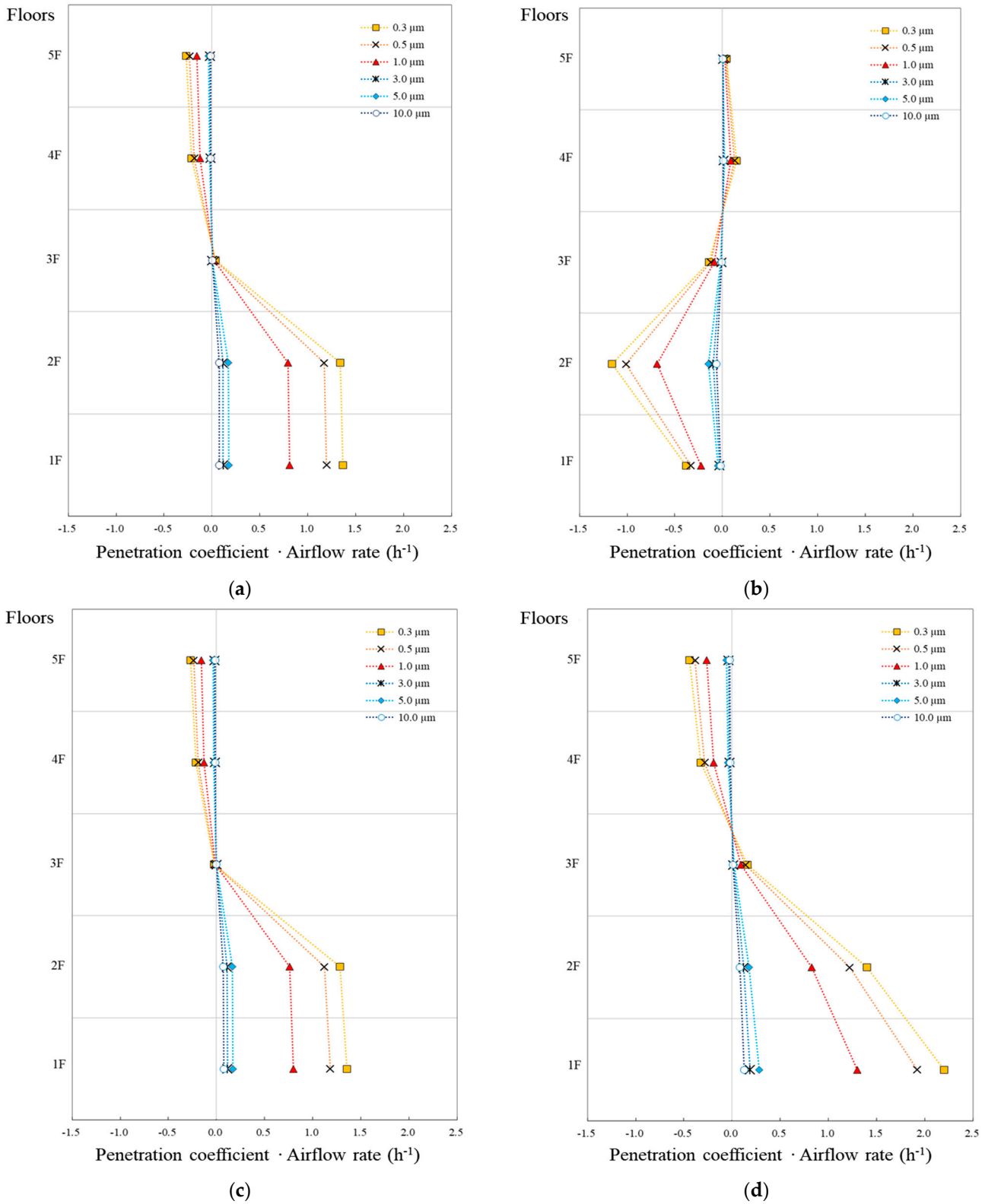


Figure 9. Amount of particle penetration through the reference-building envelope: (**a**) case 1, spring; (**b**) case 2, summer; (**c**) case 3, autumn; (**d**) case 4, winter.

In spring (Figure 9a), the number of outdoor particles transported from the first floor to the upper floor ranged from 0.08 to 1.37 h^{-1} for each particle diameter. Additionally, the inflow amounts of the 0.3, 0.5, and 1.0 μm particles were larger than those of the 3.0, 5.0, and 10.0 μm particles. The particles observed indoors were mostly fine. The number of coarse particles transported from outdoors to indoors were small, owing to the small penetration coefficient of the coarse particles.

In summer (Figure 9b), the number of outdoor particles transported from the first floor to the upper floors ranged from −0.39 to −0.02 h^{-1}. The airflow rates were lower than those in spring, and the number of particles transported from outdoors to indoors was insignificant. In addition, the number of particles in the outflow on the second floor was larger than that on the first floor. This is because part of the second floor was connected to the first floor via an atelier.

In autumn (Figure 9c), the number of outdoor particles in the inflow from the first floor and upper floors ranged from 0.08 to 1.35 h^{-1}. Similar to the results for spring, the inflow amounts of the 0.3, 0.5, and 1.0 μm particles were larger than those of the 3.0, 5.0, and 10.0 μm particles. This was attributed to the penetration coefficient of the coarse particles. It was estimated that the effect of outdoor particles was negligible on the third floor and above, that is, the neutral zone.

In winter (Figure 9d), the number of outdoor particles in the inflow from the first and upper floors ranged from 0.08 to 2.20 h^{-1}. The inflow of particles from the outdoors was significant on the first floor, where a difference between the indoor and outdoor pressures was observed. Additionally, the fine particles moved vertically through the atrium connected to the second floor. The coarse particles exhibited minimal inflow into the room owing to their small penetration coefficient.

4.3. Particle Results (II): Indoor/Outdoor (I/O) Ratio Comparison Based on Particle Diameter

Figure 10a–d shows the I/O particle concentration ratios for different particle diameters according to the indoor location in the multi-zone building. Assuming that there was no source of indoor particles and that no resuspension occurred, the I/O ratio represented the indoor contribution of particles from the outdoors, considering the inflow, deposition, and transport of particles in the building. Additionally, assuming that the concentration of outdoor particles did not change, the I/O ratio for particles was interpreted as an infiltration factor, that is, the effect of outdoor particles on the indoor particle concentration.

In all the seasons, the I/O ratios were larger for the fine particles (0.3, 0.5, and 1.0 μm) than for the coarse particles (3.0, 5.0, and 10.0 μm). This was because the coarse particles were affected by the small penetration coefficient and large deposition coefficient resulting from the particle movement. The I/O ratios for all particle sizes were larger for the lower floors than for the upper floors during spring, autumn, and winter. However, in summer, the I/O ratios for all the particles were larger on the upper floors than on the lower floors.

In spring, the I/O ratios for the particles on the lower and upper floors were 0.71 and 0.13, respectively. These results were obtained for both the fine and coarse particles. However, the I/O ratios for the coarse particles were between 0.01 and 0.10, and the contribution to the indoor particle level was smaller than that for the fine particles. The I/O ratios for all the particles in autumn and winter were similar to those in spring with similar airflow patterns.

These results indicated that the contribution of outdoor particles to the indoor particle concentration was more significant on the lower floors of the multi-zone building than on the upper floors. As the particles moved to the higher floors, their passage through multiple indoor spaces was affected by the deposition coefficient, and the overall I/O ratio for all the particles was small.

Within the same building, the I/O ratios of the particles depended on their location. The simulation results indicated that the exterior zone was directly influenced by outdoor particles, in contrast to the corridor and interior zones. The average particle I/O ratio of the exterior zone was 0.15, which was almost twice that of the corridor and interior.

Additionally, for smaller particles, the I/O ratio of the particles in the exterior zone was larger and was within the range of 0.08–0.71. This range was 1.5 times wider than that of the particle I/O ratio in the interior zone (0–0.45). However, for the coarse particles, the effect of the indoor location on the I/O ratio was insignificant. The maximum I/O ratio of the coarse particles in the exterior zone was 0.1, and that in the interior zone was approximately 0.

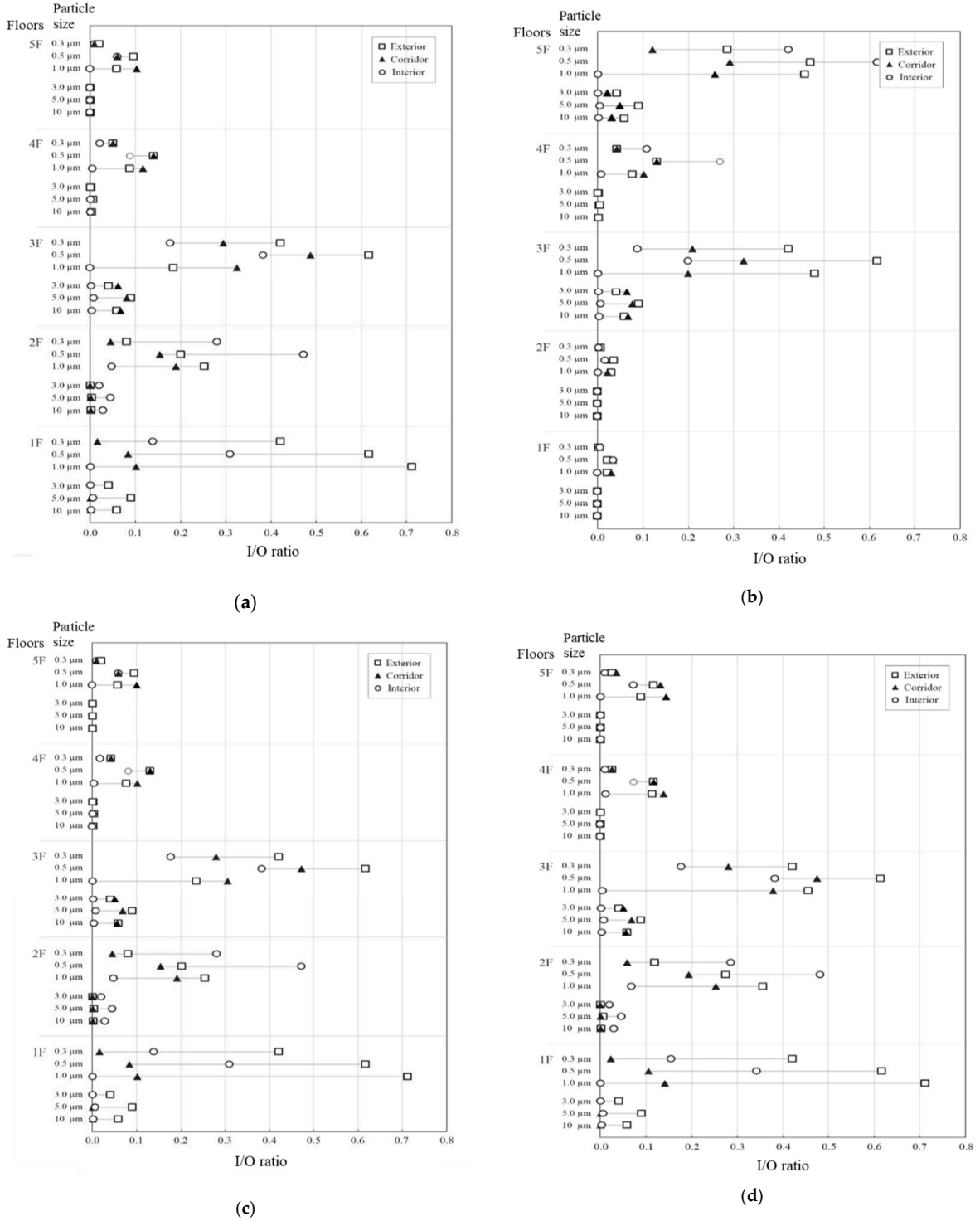


Figure 10. I/O ratio distribution profiles for the reference building: (**a**) case 1, spring; (**b**) case 2, summer; (**c**) case 3, autumn; (**d**) case 4, winter.

4.4. Particle Results (III): Indoor Particle Concentration Dependence on Outdoor PM Level

In Korea, the pollution of outdoor air is more severe in winter than in other seasons because of smog generated by combustion for heating and Asian dust storms from China. Furthermore, the infiltration rate is the highest in winter, increasing the penetration of outdoor particles. The impact of size-resolved outdoor particles was investigated for three periods in winter: normal, yellow dust storms, and smog. The mass fraction of each outdoor particle size for these periods was measured in the reference building. The total mass concentrations were assumed to be equal for the three periods, and the mass concentrations foreach particle size were calculated. The distributions of the size-resolved outdoor particle concentrations are presented in Table 3.

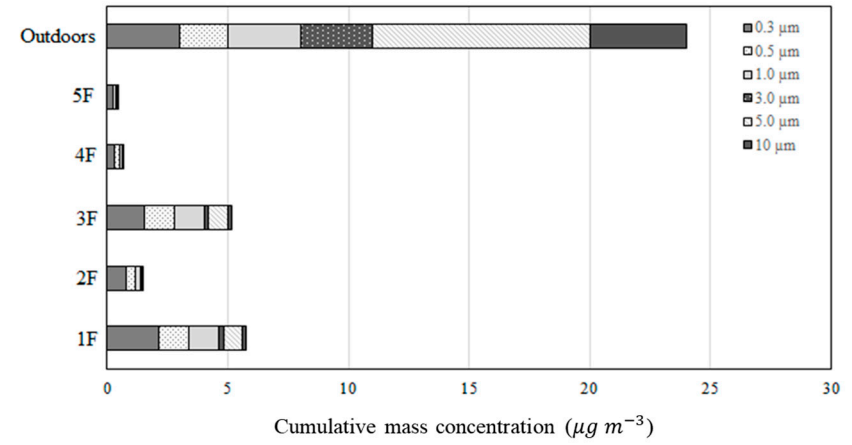
Table 3. Distributions of size-resolved outdoors particle concentrations.

Particle Diameter (μm)	Normal		Yellow Dust Storm		Smog	
	Mass Concentration (μg m^{-3})	Mass Fraction	Mass Concentration (μg m^{-3})	Mass Fraction	Mass Concentration (μg m^{-3})	Mass Fraction
0.3	19.6	0.13	8.7	0.01	18.3	0.16
0.5	13.1	0.08	8.7	0.01	18.3	0.16
1.0	19.6	0.13	34.8	0.04	15.5	0.14
3.0	13.8	0.13	7.1	0.09	9.6	0.07
5.0	41.3	0.38	38.7	0.49	39.3	0.28
10.0	18.4	0.17	27.6	0.35	24.5	0.28
Total	125.6	1	125.6	1	125.6	1

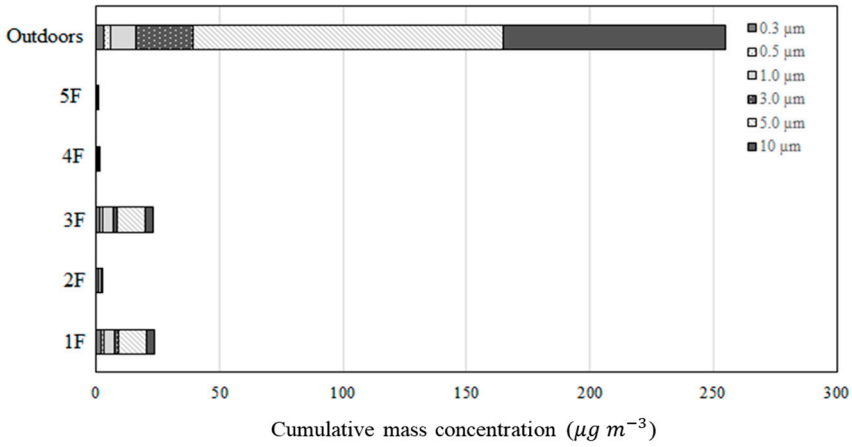
Figure 11a–c shows the indoor particle concentration in the exterior zone of each floor in the multi-zone building for the normal, yellow dust, and smog periods, respectively. The mass concentration of outdoor particles decreased in the following order: yellow dust, smog, normal. However, the indoor particle mass concentration decreased in the following order: smog, yellow dust, normal. This difference was due to the particle size distribution in the outdoor air. In particular, the mass fraction of the outdoor particles was larger in the smog period than in the yellow dust period. This reflected the dependence of the penetration coefficient on the particle-size distribution. The effect of outdoor particles on the indoor particle concentration was more significant in the smog period than in the yellow-dust period.

The indoor particle concentration on the first floor during the yellow-dust period was approximately 25 μg. However, when smog occurred, the indoor particle concentration on the first floor was approximately 50 μg, which was twice that of the former case. In particular, the mass fraction of the coarse particles in the indoor particle concentration was the highest during the yellow-dust period, whereas that of the fine particles was higher during the smog period. Considering the exposure of residents to particles, the health risks during the smog period was higher than that during the yellow-dust period.

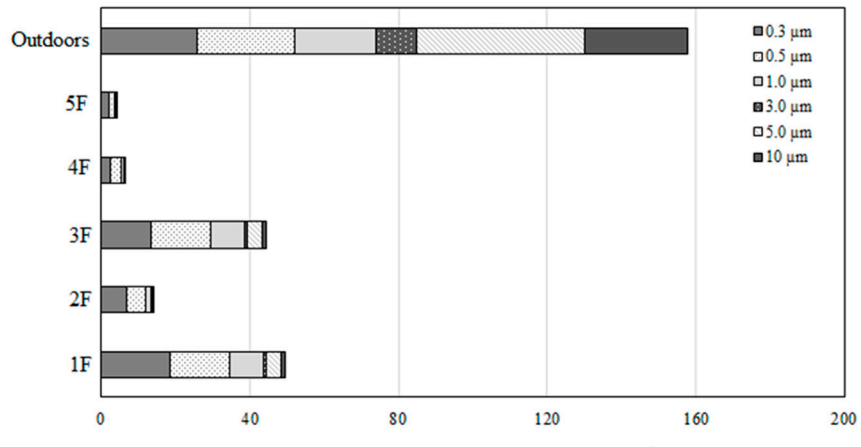
As shown in Figure 11, the mass concentration of the fine particles was higher than that of the coarse particles, indicating that outdoor coarse particles were effectively eliminated by the building envelope. Despite the effectiveness of the building envelope, it was not useful for eliminating fine particles. Therefore, it is necessary to consider whether stronger airtightness is significantly beneficial for reducing the number of penetrating outdoor fine particles. If not, further investigation is required, as shown in Figure 11, to identify active strategies that are more effective for eliminating fine particles.



(**a**)



(**b**)



(**c**)

Figure 11. Size-resolved particle mass concentrations outdoors and indoors: (**a**) normal period, (**b**) yellow-dust period, (**c**) smog period.

5. Discussion

5.1. Validity of Temporal and Spatial PM Evaluation Method

As mentioned in Section 1, the PM evaluation method should be able to estimate the amount of penetrating PM in different seasons and evaluate the indoor PM concentration

due to vertical and horizontal indoor positions. This study proposed a temporal and spatial PM evaluation method and validated it through a case study. To verify its effectiveness, the amount of penetrated outdoor PM and its distribution in vertical and horizontal positions in a reference building were evaluated for four seasons.

First, the airflow patterns for each season and their effects on the indoor PM concentration were investigated. According to the simulation conditions presented in Table 1, the effects of the wind on I/O ratio did not appear to differ significantly among the seasons. In contrast, the outdoor air temperature significantly affected the airflow patterns. In spring, autumn, and winter, when the outdoor air temperature was lower than the indoor air temperature, the outdoor air entered the lower floors and flowed to the upper floors. Considering the overall airflow path in the building, the I/O ratio was larger on the lower floors than on the upper. The outdoor air flowed in the reverse direction in the summer. The outdoor air introduced to the upper floors flowed to the lower floors and exited the building. Consequently, the I/O ratio was higher on the upper floors than on the lower floors.

The difference in the I/O ratio was also depicted by the horizontal and vertical positions. Among the exterior, corridor, and interior zones of the floors, where outdoor air primarily entered, the I/O ratio was the largest in the exterior zone. As particles entered the building, the deposition effect influenced the indoor PM concentration. This was a major cause of the difference in the I/O ratio due to the horizontal positions. In addition to the deposition effect, the building plan contributed to the difference. For instance, the partition wall surrounding the interior zone blocked incoming outdoor particles, preventing them from passing through the exterior and corridor zones. Furthermore, as these particles could only pass through the door, they could not easily reach the interior zone. The results indicated that compartmentalization was sufficiently useful for reducing the indoor particle concentrations in case studies.

5.2. Promise of Multi-Zone Simulation Method for Evaluating Indoor PM Control Strategies

The simulation results indicated that the proposed method can be used to accurately estimate the indoor PM concentrations at different indoor positions in different seasons. Accordingly, further discussion of the practical usage of the multi-zone simulation method is needed. It is necessary to investigate whether this method is feasible for evaluating the effectiveness of passive or active strategies for controlling indoor PM. Multi-zone simulations were used to assess indoor air quality [55–57]. In these studies, the building energy consumption and IAQ were estimated using CONTAM and EnergyPlus. In [57], practical usage of the model was demonstrated by evaluating the impacts of different indoor PM control strategies.

Considering the complex effects of the season and particle size on the indoor PM concentration, methods more specific than those used in previous studies are needed. In [57], the $PM_{2.5}$ and total indoor PM concentrations were evaluated without considering the spatial distribution. In the present study, only less than 10% of outdoor PM with the size larger than 1.0 μm flowed into the building. In contrast, approximately 60–70% of outdoor PM with the size less or equal to 1.0 μm flowed to several indoor positions. In spring, autumn, and winter, the indoor PM levels in the exterior zone on the first floor were higher than those at other indoor positions. This pattern indicates that more effective strategies for controlling PM in the exterior zone on the first floor are needed. The multi-zone simulation method is useful for detecting the most vulnerable indoor positions to PM and finding specific strategies to each indoor position.

5.3. Limitations

The results of the case study revealed that the temporal and spatial PM evaluation method is feasible for estimating indoor PM concentrations in different seasons. However, in this study, particles generated by indoor activities such as cooking were not considered. According to previous studies, most indoor particles originate from indoor activities when

the pollution level of outdoor air is moderate. Studies indicated that the transport of indoor-generated particles affects the PM concentrations in adjacent zones. In the future, the temporal and spatial PM evaluation method will be evaluated to determine whether changes in indoor PM concentrations due to particles originating from other zones and outdoor particle penetration can be estimated.

In addition to verifying the robustness of the proposed method, the modeling of indoor particle sources is important for the evaluation. However, this entails several challenges. First, the prediction of the number of particles generated from different indoor activities is challenging. For example, particle generation depends on factors, such as the types of oil and cooking duration. Second, the types of indoor activities during the design stage cannot be easily predicted. Because of these uncertainties, the generation of indoor particles may not be accurately estimated.

6. Conclusions

The present study investigated the effectiveness of a multi-zone model-based indoor PM evaluation method for assessing passive strategies to control indoor PM. Passive strategies can be implemented in two ways: minimizing penetration via air-tightness and blocking PM transport between different zones via compartmentalization. To evaluate the effects of both, the method should be able to estimate the amounts of penetrating outdoor particles in different seasons and the indoor particle levels at different indoor locations.

Simulations were performed in four seasons to determine the effects of the outdoor air conditions on the indoor PM level, and the I/O ratios were obtained for the exterior, interior, and corridor zones on every floor of a reference building. To establish the multi-zone model, the outdoor particle concentrations, penetration coefficient, deposition rate, and envelope leakage area were collected via field measurements in the reference building. The airflow patterns in summer differed from those in the other seasons, and their trends were similar to those of the indoor PM concentrations. The model accurately reflected the fact that the indoor PM concentration was high on floors to which outdoor air flowed. Additionally, the difference in the indoor PM concentration at different horizontal locations were accurately estimated. Overall, the indoor PM concentration was the highest among the three zones on the same floor. The results of this study indicated that the proposed method could estimate the number of penetrating outdoor particles in different seasons and the indoor particle levels at different indoor locations.

The particlesize distribution results indicated the necessity of a method to assess passive strategies for indoor PM control. As the indoor PM concentration varied with respect to the outdoor particle size and the concentration of the outdoor particles varied over time, the model should consider both the change in the outdoor particle size and its effects on the indoor PM concentration.

Author Contributions: Conceptualization, B.-H.L.; methodology, B.-H.L. and S.-H.B.; software, B.-H.L.; validation, B.-H.L.; formal analysis, B.-H.L.; investigation, B.-H.L. and S.-H.B.; resources, B.-H.L.; data curation, B.-H.L.; writing—original draft preparation, B.-H.L. and S.-H.B.; writing—review and editing, B.-H.L. and S.-H.B.; visualization, B.-H.L.; supervision, S.-H.B.; project administration, B.-H.L.; funding acquisition, S.-H.B. All authors have read and agreed to the published version of the manuscript.

Funding: This work was supported by the National Research Foundation of Korea (NRF) grant funded by the Korea government (MSIT) (No. 2022R1F1A1062895).

Data Availability Statement: Not applicable.

Conflicts of Interest: The authors declare no conflict of interest.

Nomenclature

V_k	Volume of building compartment k	m^3
Q_{mk}	Flow rate of the air that brings the outdoor PM via a pathway m in a building compartment k	$m^3\ s^{-1}$
$P_{m,i}$	Penetration coefficient of particles whose diameter is i transported via pathway m	-
$N_{out,i}$	Outdoor PM number concentration	$\#\ m^{-3}$
$Q_{k,removed}$	Removed airflow rate in building compartment k	$m^3\ s^{-1}$
$N_{k,i}$	Particle (particle diameter is i) number concentration in building compartment k	$\#\ m^{-3}$
Q_{jk}	Airflow rate from building compartment j to building compartment k	$m^3\ s^{-1}$
A_{kj}	Total surface area of deposition j in building compartment k	m^2
$v_{kj,d,i}$	Deposition velocity for deposition surface j in building compartment k	$m\ s^{-1}$
$f_{k,j,i}$	Fraction of the accumulated particles that are available for resuspension from deposition surface j to the indoor air in building compartment k	-
$\lambda_{kj,re,i}$	Resuspension rate for deposition surface j in building compartment k	s^{-1}
$B_{kj,i}$	Particle (particle diameter is i) number concentration accumulated on deposition surface j of area A_{kj}	$\#\ m^{-2}$
$G^E_{k,i}$	Number of particles (particle diameter is i) from indoor sources	$\#\ m^{-3}\ s^{-1}$
A_i	Number of penetrating particles with diameter i	h^{-1}
P_i	Penetration coefficient for particles with diameter i	-
α	Air exchange rate	h^{-1}

References

1. Sinclair, J.; Psota-Kelty, L.; Weschler, C.; Shields, H. Measurement and modeling of airbone concentrations and indoor surface accumulation rates of ionic substances at Neenah, Wisconsin. *Atmos. Environ. Part A Gen. Top.* **1990**, *24*, 627–638. [CrossRef]
2. Heil, A.; Goldammer, J.G. Smoke-haze pollution: A review of the 1997 episode in Southeast Asia. *Reg. Environ. Chang.* **2001**, *2*, 24–37. [CrossRef]
3. Hoskins, J.A. Health Effects due to Indoor Air Pollution. *Indoor Built Environ.* **2003**, *12*, 427–433. [CrossRef]
4. Zhang, Y.; Zhao, B.; Li, X. Perceived Particle Intensity: An Indicator to Evaluate Indoor Particle Pollution. *Indoor Built Environ.* **2006**, *15*, 155–164. [CrossRef]
5. Tippayawong, N.; Khuntong, P.; Nitatwichit, C.; Khunatorn, Y.; Tantakitti, C. Indoor/outdoor relationships of size-resolved particle concentrations in naturally ventilated school environments. *Build. Environ.* **2009**, *44*, 188–197. [CrossRef]
6. Chen, C.; Zhao, B. Review of relationship between indoor and outdoor particles: I/O ratio, infiltration factor and penetration factor. *Atmos. Environ.* **2011**, *45*, 275–288. [CrossRef]
7. Goossens, J.; Jonckheere, A.C.; Dupont, L.J.; Bullens, D.M. Air pollution and the airways: Lessons from a century of human urbanization. *Atmosphere* **2021**, *12*, 898. [CrossRef]
8. Weschler, C.J.; Shields, H.C.; Naik, D.V. Indoor Ozone Exposures. *JAPCA* **1989**, *39*, 1562–1568. [CrossRef]
9. Jenkins, P.L.; Phillips, T.J.; Mulberg, E.J.; Hui, S.P. Activity patterns of Californians: Use of and proximity to indoor pollutant sources. *Atmos. Environ. Part A Gen. Top.* **1992**, *26*, 2141–2148. [CrossRef]
10. Sessa, R.; Di, P.M.; Schiavoni, G.; Santino, I.; Altieri, A.; Pinelli, S.; Del, P.M. Microbiological indoor air quality in healthy buildings. *New Microbiol.* **2002**, *25*, 51–56.
11. Wang, Z.; Liu, C.; Qian, H.; Zheng, X.; Ji, W.; Zhang, X. Effect of particulate iron on tracking indoor PM2.5 of outdoor origin: A case study in Nanjing, China. *Indoor Built Environ.* **2021**, *30*, 711–723. [CrossRef]
12. Martins, N.R.; Graça, G.C. Impact of outdoor PM2.5 on natural ventilation usability in California's nondomestic buildings. *Appl. Energy* **2017**, *189*, 711–724. [CrossRef]
13. Yin, H.; Liu, C.; Zhang, L.; Li, A.; Ma, Z. Measurement and evaluation of indoor air quality in naturally ventilated residential buildings. *Indoor Built Environ.* **2019**, *28*, 1307–1323. [CrossRef]
14. Ruan, T.; Rim, D. Indoor air pollution in office buildings in mega-cities: Effects of filtration efficiency and outdoor air ventilation rates. *Sustain. Cities Soc.* **2019**, *49*, 101609. [CrossRef]
15. Abt, E.; Suh, H.; Allen, G.; Koutrakis, P. Characterization of indoor particle sources: A study conducted in the metro-politan Boston area. *Environ. Health Perspect.* **2000**, *108*, 35–44. [CrossRef]
16. Nazaroff, W.W. Indoor particle dynamics. *Indoor Air* **2004**, *14*, 175–183. [CrossRef]
17. He, C.; Morawska, L.; Hitchins, J.; Gilbert, D. Contribution from indoor sources to particle number and mass concen-trations in residential houses. *Atmos. Environ.* **2004**, *38*, 3405–3415. [CrossRef]
18. Gens, A.; Hurley, J.F.; Tuomisto, J.T.; Friedrich, R. Health impacts due to personal exposure to fine particles caused by insulation of residential buildings in Europe. *Atmos. Environ.* **2014**, *84*, 213–221. [CrossRef]

19. Wallis, S.L.; Hernandez, G.; Poyner, D.; Holmes, W.; Birchmore, R.; Berry, T. Particle matter in residential buildings in New Zealand: Part II. The impact of building airtightness, mechanical ventilation using simulated occupancy. *Atmos. Environ. X* **2019**, *2*, 100026.
20. Brittain, O.S.; Wood, H.; Kumar, P. Prioritising indoor air quality in building design can mitigate future airborne viral outbreaks. *Cities Health* **2020**, *5*, S162–S165. [CrossRef]
21. Yu, L.; Kang, N.; Wang, W.; Guo, H.; Ji, J. Study on the Influence of Air Tightness of the Building Envelope on Indoor Particle Concentration. *Sustainability* **2020**, *12*, 1708. [CrossRef]
22. Hamilton, R.S.; Mansfield, T.A. Airborne particulate elemental carbon: Its sources, transport and contribution to dark smoke and soiling. *Atmos. Environ. Part A Gen. Top.* **1991**, *25*, 715–723. [CrossRef]
23. Miller, S.L.; Nazaroff, W.W. Environmental tobacco smoke particles in multizone indoor environments. *Atmos. Environ.* **2001**, *35*, 2053–2067. [CrossRef]
24. Morawska, L.; He, C.; Hitchins, J.; Grilbert, D.; Parappukkaran, S. The relationship between indoor and outdoor airborne particles in the residential environmenet. *Atmos. Environ.* **2001**, *35*, 3463–3473. [CrossRef]
25. Wallace, L. Indoor Particles: A Review. *J. Air Waste Manag. Assoc.* **1996**, *46*, 98–126. [CrossRef]
26. Chen, A.; Cao, Q.; Zhou, J.; Yang, B.; Chang, V.W.-C.; Nazaroff, W.W. Indoor and outdoor particles in an air-conditioned building during and after the 2013 haze in Singapore. *Build. Environ.* **2016**, *99*, 73–81. [CrossRef]
27. Deng, G.; Li, Z.; Wang, Z.; Gao, J.; Xu, Z.; Li, J.; Wang, Z. Indoor/outdoor relationship of PM2.5 concentration in typical buildings with and without air cleaning in Beiling. *Indoor Built Environ.* **2016**, *26*, 60–68. [CrossRef]
28. Liao, C.-M.; Huang, S.-J.; Yu, H. Size-dependent particulate matter indoor/outdoor relationships for a wind-induced naturally ventilated airspace. *Build. Environ.* **2004**, *39*, 411–420. [CrossRef]
29. Liu, X.; Zhai, Z. Identification of Appropriate CFD Models for Simulating Aerosol Particle and Droplet Indoor Transport. *Indoor Built Environ.* **2007**, *16*, 322–330. [CrossRef]
30. Chen, Q. Ventilation performance prediction for buildings: A method overview and recent applications. *Build. Environ.* **2009**, *44*, 848–858. [CrossRef]
31. Tong, Z.; Chen, Y.; Malkawi, A.; Adamkiewicz, G.; Spengler, J.D. Quantifying the impact of traffic-related air pollution on the indoor air quality of a naturally ventilated building. *Environ. Int.* **2016**, *89–90*, 138–146. [CrossRef]
32. Liu, W.; You, R.; Chen, C. Modeling transient particle transport by fast fluid dynamics with the Markov chain method. *Build. Simul.* **2019**, *12*, 881–889. [CrossRef] [PubMed]
33. Chu, C.-R.; Yang, K.-J. Transport process of outdoor particulate matter into naturally ventilated buildings. *Build. Environ.* **2021**, *207*, 108424. [CrossRef]
34. Emmerich, S.J. Validation of multizone IAQ modeling of residential-scale buildings: A review. *ASHRAE Trans.* **2001**, *107*, 619–628.
35. Emmerich, S.J.; Nabinger, S.J. Measurement and simulation of the IAQ impact of particle air cleaners in a single-zone building. *HVACR Res.* **2001**, *7*, 223–244. [CrossRef]
36. Rim, D.; Persily, A.; Emmerich, S.; Dols, W.S.; Wallace, L. Multi-zone modeling of size-resolved outdoor ultrafine particle entry into a test house. *Atmos. Environ.* **2013**, *69*, 219–230. [CrossRef]
37. Alonso, M.J.; Dols, W.S.; Mathisen, H.M. Using co-simulation between EnergyPlus and CONTAMW to evaluate recir-culation-based, demand-controlled ventilation strategies in an office building. *Build. Environ.* **2022**, *211*, 108737. [CrossRef]
38. Chen, Z.; Chen, C.; Wei, S.; Liu, Z.; Cao, G.; Du, Y.; Li, G.; Zhu, J.; Ma, Y.; Wang, Y. Determination of key parameters (air exchange rate, penetration factor and deposition rate) for selecting residential air cleaners under different window airtightness levels. *Sustain. Cities Soc.* **2020**, *56*, 102087. [CrossRef]
39. Bekierski, D.; Kostyrko, K.B. The Influence of outdoor particulate matter PM2.5 on indoor air quality: The implementation of a new assessment method. *Energies* **2021**, *14*, 6230. [CrossRef]
40. Miri, A.; Heidari, A.; Davtalab, J.; Nosek, S.; Abdolzadeh, M. In-situ measurements of indoor dust deposition in Sistan region, Iran–the effect of windcatcher orientation. *Build. Environ.* **2022**, *219*, 109162. [CrossRef]
41. Thatcher, T.L.; Nazaroff, W.W. Effect of Small-Scale Obstructions and Surface Textures on Particle Deposition from Natural Convection Flow. *Aerosol Sci. Technol.* **1997**, *27*, 709–725. [CrossRef]
42. Eilts, S.M.; Li, L.; Pope, Z.C.; Hogan, C.J. Characterization of exhaled particle deposition and ventilation in an indoor setting. *Atmos. Environ.* **2021**, *262*, 118602. [CrossRef]
43. Mei, D.; Wen, M.; Xu, X.; Zhu, Y.; Xing, F. The influence of wind speed on airflow and fine particle transport within different building layouts of an industrial city. *J. Air Waste Manag. Assoc.* **2018**, *68*, 1038–1050. [CrossRef] [PubMed]
44. Seoul Institute. *Seoul Infographics*; Seoul Institute: Seoul, Republic of Korea, 2020; Volume 1.
45. Slovic, A.D.; Ribeiro, H. Policy instruments surrounding urban air quality: The cases of São Paulo, New York City and Paris. *Environ. Sci. Policy* **2018**, *81*, 1–9. [CrossRef]
46. Dols, W.S.; Emmerich, S.J.; Polidoro, B.J. Coupling the multizone airflow and contaminant transport software CONTAM with EnergyPlus using co-simulation. *Build. Simul.* **2016**, *9*, 469–479. [CrossRef] [PubMed]
47. Lai, A.C.K. Modeling of airborne particle exposure and effectiveness of engineering control strategies. *Build. Environ.* **2004**, *39*, 599–610. [CrossRef]
48. Sohn, M.D.; Apte, M.G.; Sextro, R.G.; Lai, A.C.K. Predicting sizeresolved particle behavior in multizone buildings. *Atmos. Environ.* **2007**, *41*, 1473–1482. [CrossRef]

49. Demetriou, D.W.; Khalifa, H.E. Evaluation of distributed environmental control systems for improving IAQ and reducing energy consumption in office buildings. *Build. Simul.* **2009**, *2*, 197–214. [CrossRef]
50. Miller, R.S. Elevator shaft pressurization for smoke control in tall buildings: The Seattle approach. *Build. Environ.* **2011**, *46*, 2247–2254. [CrossRef]
51. Walton, G.N. *AIRNET—A Computer Program for Building Airflow Network Modeling*; National Institute of Standards and Technology: Gaithersburg, MD, USA, 1989.
52. Lee, B.H.; Yee, S.W.; Kang, D.H.; Yeo, M.S.; Kim, K.W. Multi-zone simulation of outdoor particle penetration and transport in a multi-story building. *Build. Simul.* **2016**, *10*, 525–534. [CrossRef]
53. Chao, C.Y.; Wan, M.; Cheng, E.C. Penetration coefficient and deposition rate as a function of particle size in non-smoking naturally ventilated residences. *Atmos. Environ.* **2003**, *37*, 4233–4241. [CrossRef]
54. Elimelech, M.; Gregory, J.; Jia, X.; Williams, R.A. Introduction. In *Particle Deposition & Aggregation*, 1st ed.; Butterworth-Heinemann: Oxford, UK, 1995; Volume 1, pp. 3–5.
55. Dols, W.S.; Milando, C.W.; Ng, L.; Emmerich, S.J.; Teo, J. On the Benefits of Whole-building IAQ, Ventilation, Infiltration, and Energy Analysis Using Co-simulation between CONTAM and EnergyPlus. *J. Phys. Conf. Ser.* **2021**, *2069*, 012183. [CrossRef]
56. Heibati, S.; Maref, W.; Saber, H.H. Assessing the energy, indoor air quality and moisture performance for a three-story building using an integrated model, part two: Integrating the indoor air quality, moisture and thermal comfort. *Energies* **2021**, *14*, 5648. [CrossRef]
57. Underhill, L.J.; Dols, W.S.; Lee, S.K.; Fabian, M.P.; Levy, J.I. Quantifying the impact of housing interventions on indoor air quality and energy consumption using coupled simulation models. *J. Expo. Sci. Environ. Epidemiol.* **2020**, *30*, 436–447. [CrossRef] [PubMed]

Disclaimer/Publisher's Note: The statements, opinions and data contained in all publications are solely those of the individual author(s) and contributor(s) and not of MDPI and/or the editor(s). MDPI and/or the editor(s) disclaim responsibility for any injury to people or property resulting from any ideas, methods, instructions or products referred to in the content.